Nigerian Journal of Solar Energy, Vol. 25, 2014.


# Impact of Changes in Diurnal Shortwave Solar Radiation on Air Pressure and Relative Humidity at Ilorin, Nigeria

*Ajibola, T.B., Akoshile, C.O. and Fatigun, A.T.
Department of Physics, University of Ilorin, Ilorin, Nigeria.

***Abstract*** *- Solar Radiation incident on the Earth surface passes through the earth's atmosphere and undergoes absorption, transmission and reflection. The fluctuation in intercepted solar radiation has effect on both living and non-living beings on the earth and is therefore worth examining. In this study, time dependent measurements of incident solar radiation flux, relative humidity (RH) and pressure using radiometers, pressure sensors and relative humidity measuring devices respectively, were made at Ilorin, Nigeria, bearing Lat. $8^0$ 32' N, Long.$4^0$ 34' E. in the Tropics for a period of a solar cycle. The study showed that the shortwave (SW) global radiative flux has maximum in the day time between the hours of 1200 and 1400 Local Time (LT) while the RH maximum occurred at early dawn between 0600LT and 0900LT daily and minimum around 1800LT. The atmospheric pressure has 2 minima and 2 maxima per day. The plot of RH against SW gives a skewed Gaussian. The plot (RH-SW) gave a linear relationship of slope 9.79 X $10^{-2}$ %/$Wm^{-2}$ before the maximum and 4.56 X $10^{-2}$ %/$Wm^{-2}$ after the maximum with respective correlation coefficients (R) of 0.97 and 0.90. This implies that the maximum is approached sharply at about twice the rate of relaxation after the maximum before sunset. Pressure against SW plot gave a quadratic relationship before the turning point with R of 0.99 and a linear relationship after the maximum of gradient 6.6 X $10^{-3}$ mbar/ (W/m2) and R of 0.98. Pressure against RH gave a quadratic relationship with R = .98. Daily RH has a minimum of 70% and an average of 90% in the raining season and 20% in the dry season. When the SW is high, RH dropped and Pressure increased.*

***Keywords: shortwave solar radiation, relative humidity, climate change, solar activity, pressure***

## 1. INTRODUCTION

Solar electromagnetic radiation is recognized as the primary and almost the sole source of energy for myriads of physical and biological processes on the planet Earth. Shortwave radiation which is a component of the solar radiation supplies most significant energy needed for all forms of life on Earth (Acra, 1990).

This is a study of the relationship between global shortwave solar radiation, atmospheric pressure and relative humidity for a period of 11 years between 1995 and 2005, using data obtained from measurements at the Baseline Surface Radiation Network (BSRN) Station at the University of Ilorin, Ilorin.

Shortwave solar radiation in the wavelength range of 0.25 to 4 μm provides about 99% of the total incoming solar radiation (Mark, 1999). The received daily radiation per unit area peaks at about noon before reducing to a minimum as sunset approaches. The magnitude of the intercepted radiation is a function of time of day and time of year for any given latitude (McVeigh, 1976). The incoming shortwave solar radiation reaching the surface of the earth comes in as direct and diffuse radiation (Kumar et. al, 1997; Mark, 1999). Consequently, the Earth's climatic system is constantly adjusting itself in a way that tends toward maintaining an energy balance between the energy reaching the earth from the sun and the energy that goes out from the earth back into space, in what is known as the earth's "radiation budget" (Wilson, 2009). The relative humidity is a measure of the actual amount of water vapour in the air when compared with the capacity of water vapour that the atmosphere can hold at saturation; and atmospheric pressure is the amount of force per unit area exerted by the atmosphere on the objects on which it rests. That weight depends on density, temperature and composition of the atmosphere, which is not constant due to wind movement. Changes in the atmospheric pressure have consequent effects on weather. At the sea level, the atmospheric pressure is on the average 101.3 kPa. Atmospheric pressure decreases with height. Consequently, it is reasonable to measure SW, RH and pressure as the time changes at a latitudinal and longitudinal location. The long time variation of these parameters (in the measurements made) at a location dictates the description of the observed weather and climate of that location and this is what is being done at and concerning Ilorin. The result will be a good description of this geographical location and its surrounding latitude in the tropics.

## 2. MATERIALS AND METHOD

### 2.1. Measurements

Radiometer converts incoming solar radiation to electric current in photo sensors due to release of

*Corresponding author Tel: +234-8033840127
Email: bentai@unilorin.edu.ng

electrons and production of electromotive force (emf) in the millivolt range. The voltage output is then converted to optical absorption coefficient via a reduction process using the sensitivity factor provided by the manufacturer of the instrument (Miskolczi et al., 1990). It is usually desirable for radiometers to respond equally to equal amounts of energy at all wavelengths over the wavelength range of the radiation being measured.

Eppley Precision Spectral Pyranometer, (PSP) was used to measure the solar global, sun and sky, radiation in selected sw wavelength bands. The pressure sensor employed in this study is the Vaisala HUMICAP180 that has capacitive relative humidity (RH) sensor as well. The capacitance of the RH sensor changes with humidity of the air. The sensor is powered by a 12 volt battery. The data is compatible with the CR10 data logger used to store the data at operating temperature range of – 40 $^{0}$C to 60 $^{\circ}$C. The current consumption is less than 4 milliampere when operating with a 12 volt power source. The RH accuracy is within + 3%, for average value of 0 to 90%.

The pyranometer is calibrated regularly, sometimes at the Air Resources Laboratory in Boulder, Colorado, USA Eppley Laboratory or at Davos, Switzerland to ensure compliance to BSRN requirement and reliability. The instruments are positioned on a flat platform at a height 12.91m on top of the Physics Department building in the University of Ilorin. The site ensured optimum exposure of sensors to incoming radiation from sunrise to sunset in compliance with BSRN (Miskolczi et al., 1990) recommendation. Data generated by the sensors were stored in the CR10 data logger storage Module, serial No. 449. 10, with PC208 data logger support software provided by Campbell Scientific, Inc., Logan, U. S. A.

### 2.2. Method of Data Analysis

Data quality is ensured by eliminating spurious errors that could arise from incidental shading, by discarding observations for which shortwave global radiation is less than 20Wm$^{-2}$ in the data processing. The data assembled on minute-by-minute basis was used to generate hourly and daily averages from which weekly and monthly averages were obtained.

The result was used to obtain the diurnal trend. A day's data assembled on minute by minute basis has 1440 sample points and average value of

$$X_{av} = \frac{1}{n}\sum_{i=1}^{n} X_i \qquad (1)$$

where Xi is the parameter of interest amongst shortwave radiation, relative humidity or pressure and n is the number of minutes from 00:00 hour to make an hour, a day or a week as the case may be.

Shortwave solar radiation becomes minimum at dusk and remains minimal throughout night hours before starting to rise at dawn and reaching its maximum in the day time. The daily average data has 365 points (or 366 in leap year ).

## 3. RESULTS AND DISCUSSION

### 3.1. Daily and Weekly behaviour

It is observed generally that in any year, the radiation has two significant maxima and minima of differing magnitudes. In Figure 1a, these features are more conspicuous in the year 2000, which was found to be the year of high solar activity. This agrees with the findings of Babatunde and Aro (1990). The separation in time between annual maxima lies between 5½ to 6 months a year and similarly the minima for each year. The exact location in the year appears to be drifting by about a month not commencing or finishing on exactly the same month of the year. The two maxima occurred about April and September corresponding to the time the rain is just coming in and "washing" the harmattan dust off from the air and when the rain is about leaving with the air washed clean with clearness of sky. The maximum in July/August shows that during this period, despite the cloud cover over Ilorin, most of the atmospheric dust is washed off and whenever the cloud gives way to sunshine during the day, the sun radiation influx is severe. There is however heavy reflections of the incoming Shortwave Solar Radiation by persistent moving cloud.

Weekly variation is obtained by finding the weekly average of 7 consecutive days' data, which is equal to 1 week. Array of 52 consecutive weeks are produced whose average makes the year's data points shown in Figure 1b. Each week value depends on the prevalent weekly atmospheric conditions. Figure1b revealed that the maximum values occurred about week 12 (in the month of March) and week 42 (in October). Each maximum is followed by a minimum with one occurring about April, week 18 and the other in November, week 46, of each year.

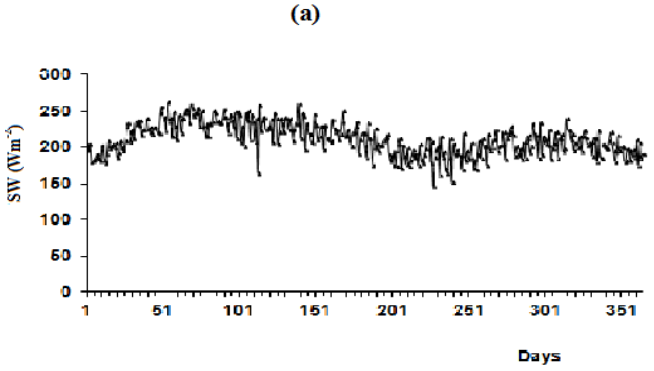


Fig. 1a: Daily Average SW (Wm-2) Plots averaged over the years 1995 to 2005

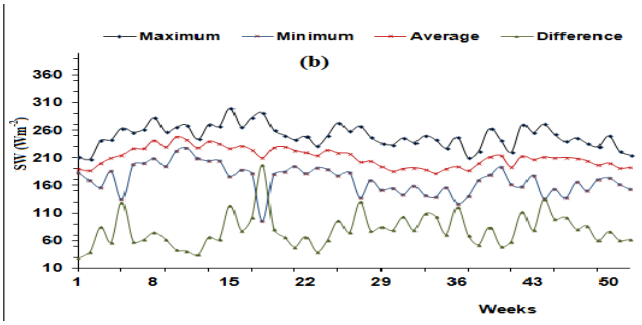


Fig. 1b: Weekly average SW (Wm-2) Plots of maximum, Average, Minimum, and Difference between Maximum and Minimum (in that order from top to bottom) compared over the solar cycle

The Relative Humidity (RH) depends strongly on the water content in the atmosphere which has saturation point. This is dependent on Pressure which also depends on the amount of incident solar radiation on the earth because the incident radiation heats the earth which changes its temperature at global and local perspective and varies with time.

The Relative Humidity plots showed that the RH was high and relatively constant at night time from immediately after midnight until about 0700LT in the morning. It is followed by dropping at sunrise to its daily minimum at about the 1700LT, as shown in Figure 2a. Following this, it begins to rise again until the following midnight. The studies revealed further that the day time values fluctuate as it approaches the minimum. April and September data showed that the minimum RH in September is close to 70% while the minimum in April is close to 20%. The seasonal variation is thereby revealed showing higher RH values in the raining season and lower values in the dry season.

Hourly averaging produces a pattern of maximum from 0000LT until to about 0800LT and then fall to a minimum at about 1800LT which again is followed by a rise to 0000LT before repeating the process to maximum the following midnight, Figure 2c. The daily averaging plot of relative humidity shows dependence on the season and prevailing daily atmospheric conditions, Figure 2a. RH has annual minimum between January and March and then rises to reach maximum between July and September followed by a continuous drop to the beginning of the following year.

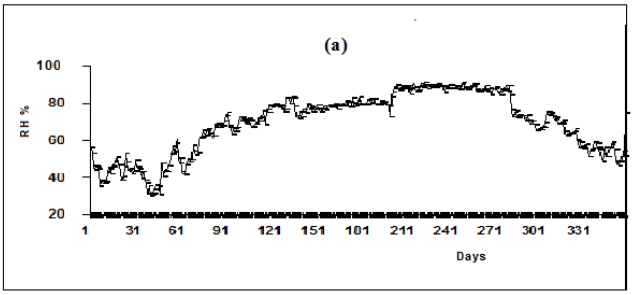


Fig. 2a: Daily Averages of RH (%) Plots for the years 1995 to 2005

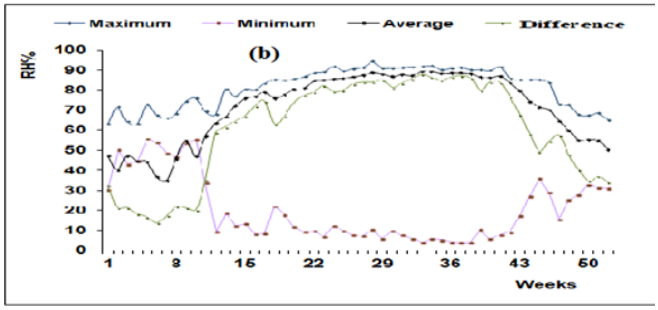


Fig. 2b: Weekly plots of Maximum, weekly Average, Minimum, and Difference between Maximum and Minimum (in that order from top to bottom) compared over the solar cycle

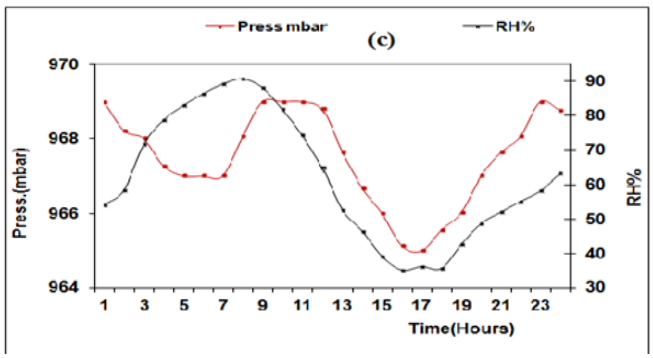


Fig. 2c: Diurnal Plots of Atmospheric Pressure (Mbar; Curve With First Minimum) and RH (%)

Average daily RH has its minimum early in the year as does the difference between maximum and minimum values as shown in Figure 2a. The weekly average plot is derived from the daily average plot and has similar features, The information deductible from the daily values are not exactly the same as that from weekly values on a long term consideration and weekly values are to be preferred over monthly values. Since seasons cover several weeks and months, it provides a means of assessing seasonal variation which covers a few months with a few data points of maximum 12 when there is no seasonal change in the year to a minimum of 12 weekly points in 3 months. Therefore weekly averaging can give better definition of seasonal changes than monthly ones.

Figure 2c shows that Pressure comes to minimum value at about 0500LT and then begins to increase until around 1000LT before commencing to drop until around 1500LT. This is followed by another increment from attained minimum to the next maximum that occurs at about 2300LT. Daily average plot of Pressure over a year showed that higher values are obtained in the raining season, between the months of June and September as shown in Figure 3a. The difference of between 1 and 2 mbar in the pressure values is relatively Figure 3c except for some spikes that mainly occurred between January and June before the rains become heavy. The trend of both minimum and maximum daily average atmospheric pressure is similar.

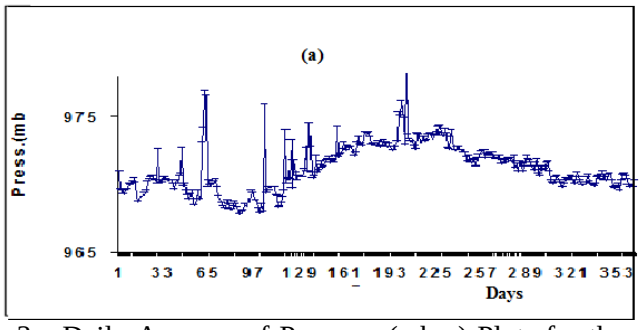


Fig. 3a: Daily Average of Pressure (mbar) Plots for the years 1995 to 2005

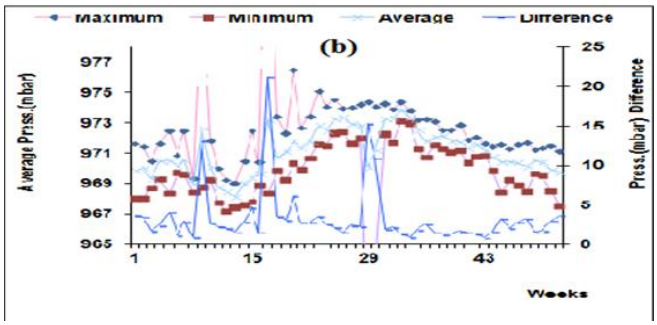


Fig. 3b: Weekly average pressure plots of Maximum, Average, Minimum and Difference between Maximum and Minimum compared (in that order from top to bottom) over the solar cycle

### 3.2. Correlations Between Parameters

#### 3.2.1. Shortwave and Relative Humidity

It is observed generally that in any year, the radiation (Liu et al., 2008) has two significant maxima and minima of differing magnitudes, as shown in Figure 1a, these features are more conspicuous in the year 2000, which was found to be the year of high solar activity. This agrees with the findings of Babatunde and Aro (1990). Figure 4 shows how the relative humidity changes with the shortwave radiation from sunrise to sunset and especially about when the SW reaches its maximum. The SW first increases and then decreases while the RH gives the opposite behavior. The nature of the change before the maximum shows some linear drop while the later growth is not linear relative to SW.

The trend in the plot of daily SW against RH is analyzed by breaking the curve into pre-peak, about peak and post peak for the corresponding values in time of Figure 4. The pre- peak is linear and has negative slope shown in Figure 4a. Equation 2 below gives the pre-peak linear relationship between SW and RH

$$y = -0.0979x + 92.773 \quad (2)$$

with correlation coefficient, R = 0.97.

where y = RH and x = SW, for the general equation y = mx + c.

The relationship for about the peak is exponential equation 3.

$$y = 27.275\, e^{0.0017x} \quad (3)$$

also with correlation coefficient, R = 0.97

Shortwave and Relative Humidity were found to also have a good correlation with each other as shown in Figures 4a, b and c. Figure 4c gives the cyclic daytime relationship between the SW and RH. The rate of decrement in RH for the morning and early noon hour's pre-peak region is much slower than the exponential rate of growth of RH post-peak of RH against SW. This implies that the incoming of SW makes the RH drop while RH rises more rapidly as the SW disappears.

#### 3.2.2 Shortwave and pressure

The plot between Pressure and SW is shown in Figure 5. Figure 5a and b are plots for about peak and post peak relationship of Pressure against SW for corresponding times in a sample day 1 of year 2000.The daily behavior of the parameters for corresponding time of measurement being compared shows behavior that is not observed in weekly or annual pattern. In the case of pressure P and SW, it was non-linear before maximum SW flux and linear after which is opposite to the behavior of RH-SW. Before attaining the peak value, the pressure bore a quadratic relationship with shortwave solar radiation Figure 5. (a), and a linear relationship after the attainment of the peak value (Figure 5. (b). The equations of these relationship are given as equations (4) and (5):

$$y = -6\times10^{-6}x^2 + 0.0016x + 968.93 \quad (4)$$

with correlation coefficient, R = 0.98.

$$y = 0.0066x + 964.49 \quad (5)$$

with correlation coefficient, R = 0.98, where y is P and x is SW.

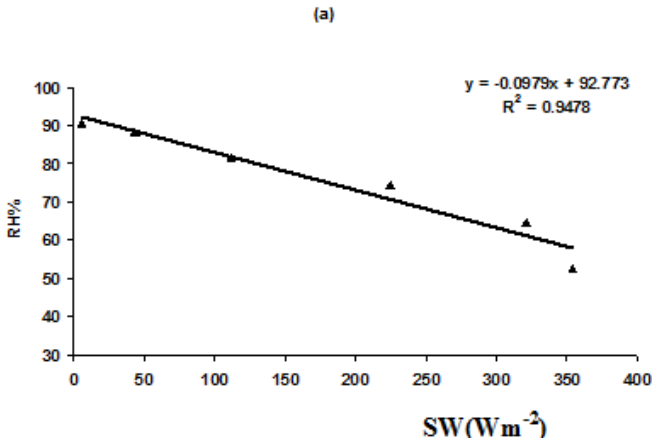


Fig. 4a: Pre-Peak and Post-Peak Correlation between Relative Humidity (%) and SW ($Wm^{-2}$) for day 1 year 2000, a year of high solar activity, with linear trend (a), exponential trend

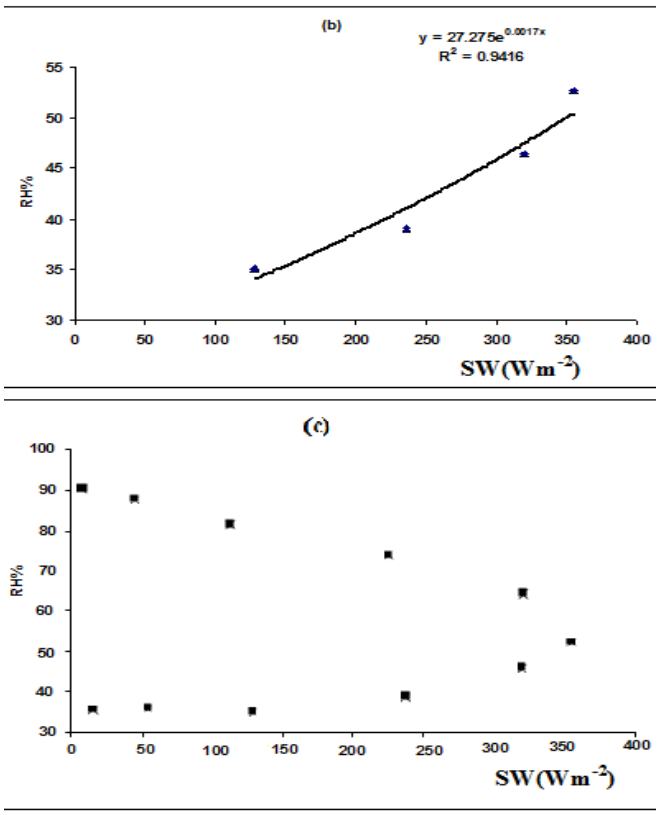


Fig. 4b,c: Pre-Peak and Post-Peak Correlation between Relative Humidity (%) and SW ($Wm^{-2}$) for day 1 year 2000, a year of high solar activity, with linear trend (b) and the daytime scatter plots of Relative Humidity (%) against SW ($Wm^{-2}$) (c)

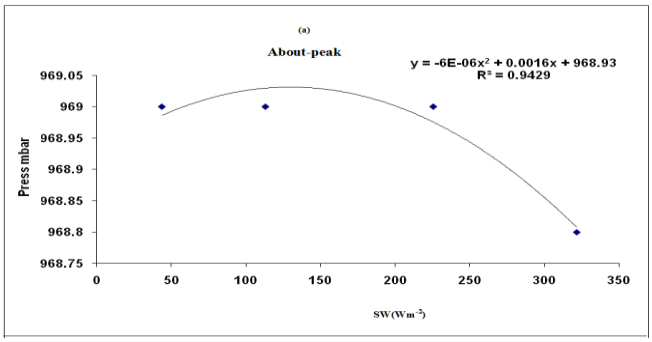


Fig. 5: Correlation between pressure (mbar) and SW ($Wm^{-2}$) (a) about-peak

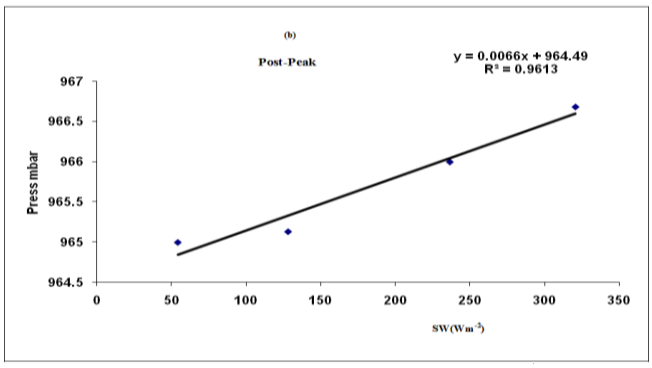


Fig. 5: Correlation between pressure (mbar) and SW ($Wm^{-2}$) (b) post-peak for sample day 1 year 2000

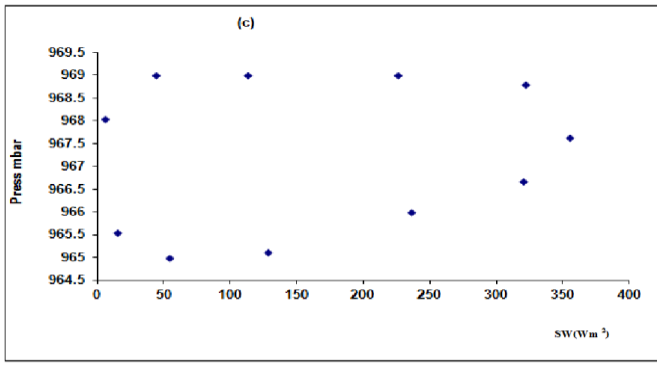


Fig. 5: Correlation between pressure (mbar) and SW ($Wm^{-2}$) (c) the daytime scatter-plots of pressure (mbar) and SW ($Wm^{-2}$)

### 3.2.3 Relative Humidity and pressure

It is also useful to see how Pressure and Relative humidity relate. In a day, relative humidity has one maximum and one minimum, while pressure has two of each. Figure 6 showed that there is a quadratic relationship between pressure and RH, using the day time data for a representative day. The quadratic equation is

$$y = -0.0023x^2 + 0.3519x + 955.63 \quad \ldots \quad (6)$$

with correlation coefficient, R = 0.99, where y is Pressure and x is RH. Such comparison can only be done by examining the behavior of the patterns for a single day at a time. The behavior about the turning point, before and after, are not the same, and a sample day was selected for this comparison as shown in the figure. A year of high solar activity was selected to select the day

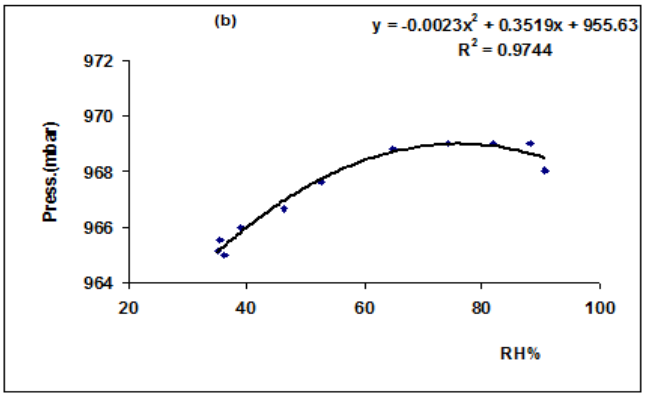


Fig. 6: Daytime Correlation between Pressure (mbar) and RH (%) for concurrent time period of a day

## 4. CONCLUSION

The study of effect of SW on RH and Atmospheric pressure is presented in this study. On the daily behavior, there is a linear relationship between SW and RH before the curves turning point, exponential correlation after the turning point and quadratic polynomial relationship about the turning point with correlation coefficients. The

rate of decrement in RH for the morning and early noon hours before the turning region, is much slower than the exponential rate of growth of RH at the post- turning of RH-SW range. Pressure has both a maximum and a minimum between sunrise and sunset. Before attaining the peak value as shown in the P-SW plot, the pressure-drop was quadratic with correlation coefficient of 0.99, while it increased linearly after the attainment of the peak value. The pressure decreased as the intensity of the shortwave increased. The daily average pressure depends on the season and corresponding changes.

Comparative study of the parameters considered for day-time showed that the maximum value of SW occurred slightly earlier in time than the minimum of RH but the maximum of RH precedes the maximum of the SW. As more radiation comes in, the relative humidity begins to drop in value. Thus, the average RH values and the difference, between its Maximum and Minimum values, have their minimum occurring early in the day. The seasonal variations of pressure were observed from the Daily average plot of Pressure over a year which showed that higher values occurred in the raining season, between the months of June and September. The daily Pressure fluctuation is generally less than 4 mbar per day. It seems to be low between January and ending of February, but large fluctuations in Pressure occur between the months of February and May in the year. These observable demarcations show the existence of three seasons (Rodriguez-Puebla et al., 2008), namely the Harmattan season, Dry season and the Rainy season (Pinker et al., 2006). In the raining season, fluctuations lie between 1 and 3 mbar. These correlated relationships are useful for understanding the climate, climate change (IPCC., 2007) and weather forecasting.

## ACKNOWLEDGEMENT

We wish to acknowledge the support received by Baseline Surface Radiation Network (BSRN) Station, Ilorin through Professor R. T. Pinker of the University of Maryland, USA and Prof. T. O. Aro (now of Bowen University, Iwo, Nigeria, initially of the University of Ilorin) and the University of Ilorin, Ilorin, Nigeria.

## REFERENCES

Acra, A., Urdi, M., Mu'allem, H., Karahagopian, Y. and Raffoul, Z. (1990). Water Disinfection by Solar radiation, Assessment and Application, International Development Research Centre (IDRC - Canada).

Akoshile, C. O., Garnesh, S., Ajibola, T. B., Babatunde, E.B., Willoughby, A.A., Falaiye, O.A, Adimula, I.A., Aro, T.O. and Pinker, R.T. (2004. Relative Humidity Variations At Ilorin, Nigeria; Edited Conference Proc.NIAE: Vol.26, pp 236-240.

Babatunde, E. B., Akoshile, C. O., Falaiye, O. A., Willoughby, A.A., Ajibola, T.B., Adimula, I.A. and Aro, T.O. (2009). Observation bio-effect of SW-global solar radiation in Ilorin in the tropics, Advances in Space Research, 43, 6, pp. 990-994., Publisher: ELSEVIER.

Babatunde, E. B., Akoshile, C. O., Falaiye, O. A. and Ajibola, T. B. (2013). Global Solar Radiation. Annual Profile, Causes and Seasonal Effects, at Ilorin, Nigeria, Covenant Journal of Physical and Life Sciences (CJPL) Vol. 1,1, p. 9-13.

Eppley Laboratory, Inc., 12 Sheffield Avenue, Newport, (1999). RI 02840,401, pp. 847-1020. http://www. Eppleylab. Com.

Intergovernmental Panel on Climate Change (IPCC) (2007). Summary of Policymakers, in Climate Change 2007: The Physical Science Basis: Working Group I Contribution to the Fourth Assessment Report of the IPCC, edited by S. Solomon et al., pp. 1-18, Cambridge Univ. Press, New York.

Kumar, L., Skidmore, A.K. and Knowles, E. (1997). Modeling topographic variation in solar radiation in a GIS environment, International Journal for Geographical Information Science, 11, 5, pp. 475-497.

Liu, H., and Pinker, R. T. (2008). Radioactive fluxes from satellites: Focus on aerosols, J. Geophys. Res., 113.

Mark, A. M. (1999). Japan Association of Remote Sensing, 1996, Spectral Characteristics of Solar radiation. School of Natural Resource Sciences, University of Nebraska-Lincoln. html.

McVeigh, J.C. (1976). Sun power -- an introduction to the application of solar energy. Pergamon Press, New York, NY, USA. 208p.

Miskolczi, F. et. al. (1990). High Resolution Atmospheric Radiance- Transmittance Code, Met. and Env. Sci. World Sci. Pub. Co., 743- 790.

Miskolczi, F. (1992). Modeling of Downward Surface Longwave Flux Density for Global Change Applications: Preliminary Results. International Astronomical Federation.

Pinker, R. T., Zhao, Y., Akoshile, C., Janowiak, J. and Arkin, P. (2006). Diurnal and seasonal variability of rainfall in the sub-Sahel as seen from observations, satellites and a numerical model, Geophys. Res. Lett., 33.

Rodriguez-Puebla, C., Pinker, R. T. and Nigam, S. (2008). Relationship between downwelling surface shortwave radiative fluxes and sea surface temperature over the tropical Pacific: AMIP II models versus satellite estimates, Ann. Geophys., 26(4), 785-794.

Wilson, S.R., Zhang, T., Wielicki, B. A., Stackhouse, P. W. and Hinkelman, L. M. (2009). Surface insolation trends from satellite and ground measurements: Comparisons and challenges, J. Geophys. Res. Atmosphere, 114, D10.